1964

A study of the relationships between wear and deformation for carbide cutting tools

John J. Burbridge
Lehigh University

Abstract

During a cutting operation on a lathe, a bulge usually forms on the flank of a cemented carbide tool. This bulge represents some type of deformation process that occurs in the tool. The actual relationship of this deformation with the wear processes that are known to occur in cutting with cemented carbides had not been explored. This thesis attempts to show how deformation contributes to these wear processes and how deformation is related to flank wear as represented by the general wear curve. It is shown that while actual deformation in cemented carbides increases steadily with increasing flank wear, interference between the flank of the tool and the workpiece prevents the deformation on the flank of the tool to increase past a certain point of flank wear. The interference between the bulge on the flank of the tool and the workpiece is a cause of flank wear.

A STUDY OF THE RELATIONSHIPS BETWEEN WEAR AND DEFORMATION FOR CARBIDE CUTTING TOOLS

by
John Joseph Burbridge, Jr.

A Thesis

Presented to the Graduate Faculty

of Lehigh University

in Candidacy for the Degree of

Master of Science

Lehigh University

1964

This thesis is accepted and approved in partial fulfillment of the requirements for the degree of Master of Science.

21 MAY 1964

Date

George E. Kane

Professor in Charge

[signature]

Head of the Department

Acknowledgments

I would especially like to thank Professor George E. Kane for his advice and guidance. I would also like to thank Mr. Gilbert Zambelli and the late Mr. Raymond Grund for their help in the experimental work.

Table of Contents

List of Figures

Abstract

During a cutting operation on a lathe, a bulge usually forms on the flank of a cemented carbide tool. This bulge represents some type of deformation process that occurs in the tool. The actual relationship of this deformation with the wear processes that are known to occur in cutting with cemented carbides had not been explored. This thesis attempts to show how deformation contributes to these wear processes and how deformation is related to flank wear as represented by the general wear curve. It is shown that while actual deformation in cemented carbides increases steadily with increasing flank wear, interference between the flank of the tool and the workpiece prevents the deformation on the flank of the tool to increase past a certain point of flank wear. The interference between the bulge on the flank of the tool and the workpiece is a cause of flank wear.

Introduction

This thesis is concerned with the deformation process in cemented carbide cutting tools and the relationships that exist between the process of deformation and the various mechanisms of wear. This experimental work was done in conjunction with the work conducted at Lehigh University under National Science Foundation Grant - 24000, "Deformation in Sintered Carbide".

Vieregge (1) contends that there are five mechanisms of wear in a cutting operation. The rates of each of these mechanisms with speed or temperature is seen in Fig. 1.

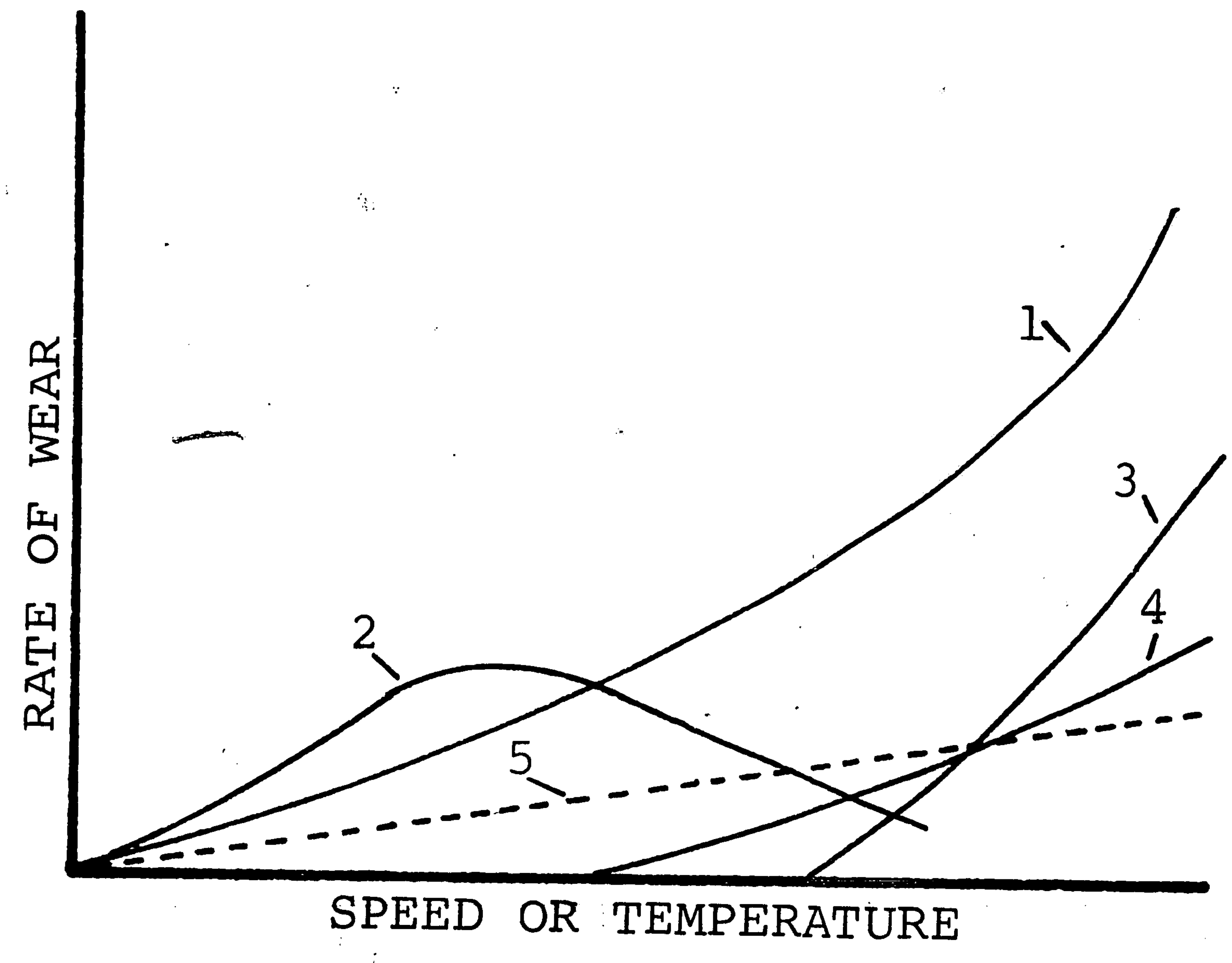

Fig. 1 - A Qualitative Indication of the Relative Influence of Five Discrete Mechanisms of Tool Wear. (Adapted from Vieregge (1)).

The first mechanism is abrasion or mechanical interference between the chip, workpiece and the tool. This process occurs both at the face and the flank of the tool. On the face, it is the chip that interferes with the tool. The flank of the tool interferes with the workpiece.

The second mechanism of wear is the formation of the built-up edge. The built-up edge affects the rate of wear on the flank of the tool at low temperatures. Above a certain temperature or speed, the built-up edge no longer forms. Since the primary concern here is with carbides and the speeds are fairly high, the built-up edge should not be encountered.

The third mechanism is diffusion of the tool material into the underside of the chip. This mechanism does not become important until a substantial temperature is reached in the cutting process.

The fourth mechanism of wear is described as oxidation or chemical decomposition of the tool material. This mechanism is shown to achieve significance at lower temperatures than that designated for diffusion.

The fifth mechanism is deformation. Vieregge represents the rate of plastic flow or deformation as remaining constant as the speed or temperature is increased. Vieregge is not sure of this relationship and represents it as a dashed line. Colwell (2) points out that there is probably a certain temperature at which the rate of deformation will increase sharply. He also says that there is very little evidence to support any conclusions concerning deformation.

Trent (3) has noticed deformation on the flank of a cemented carbide tool. He states that when the feeds and speeds are high, the tip of a cemented carbide tool becomes deformed under a compressive load, and the flank of the tool is bulged toward the workpiece. An illustration of this deformation is shown in Fig. 2.

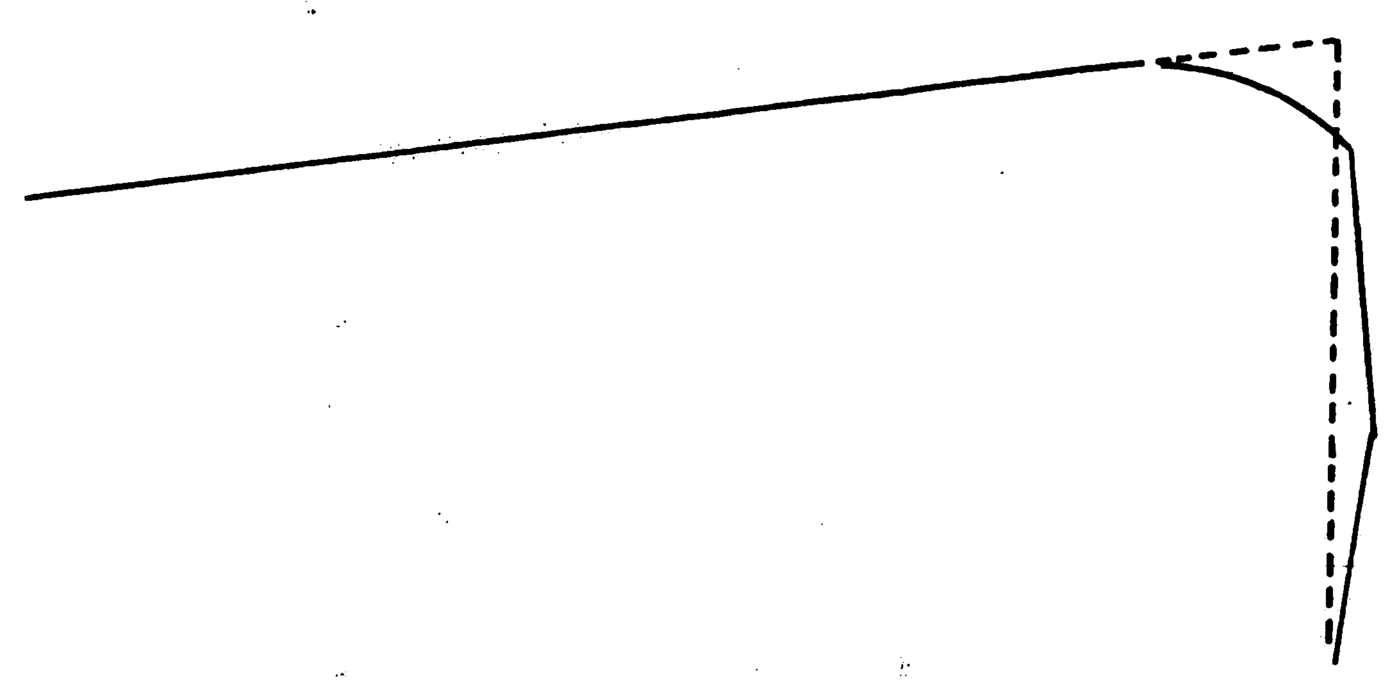

Fig. 2 - Deformation of a Cemented Carbide Cutting Tool as Seen by Trent (3).

In Fig. 3 the general wear curve is shown. This curve shows the height of flank wear as a function of length of cut or time. Black (4) explains this curve in the following manner. At the beginning of a cut, the curve shows a rapid development of the flank wear. This is due to the breaking in of the tool. Then there is a gradual but moderate increase in flank wear until a point of inflection is reached. Beyond this point, failure of the tool is imminent. The region beyond the point of inflection is termed by Chao and Trigger (5), the temperature-sensitive region. The goal of this

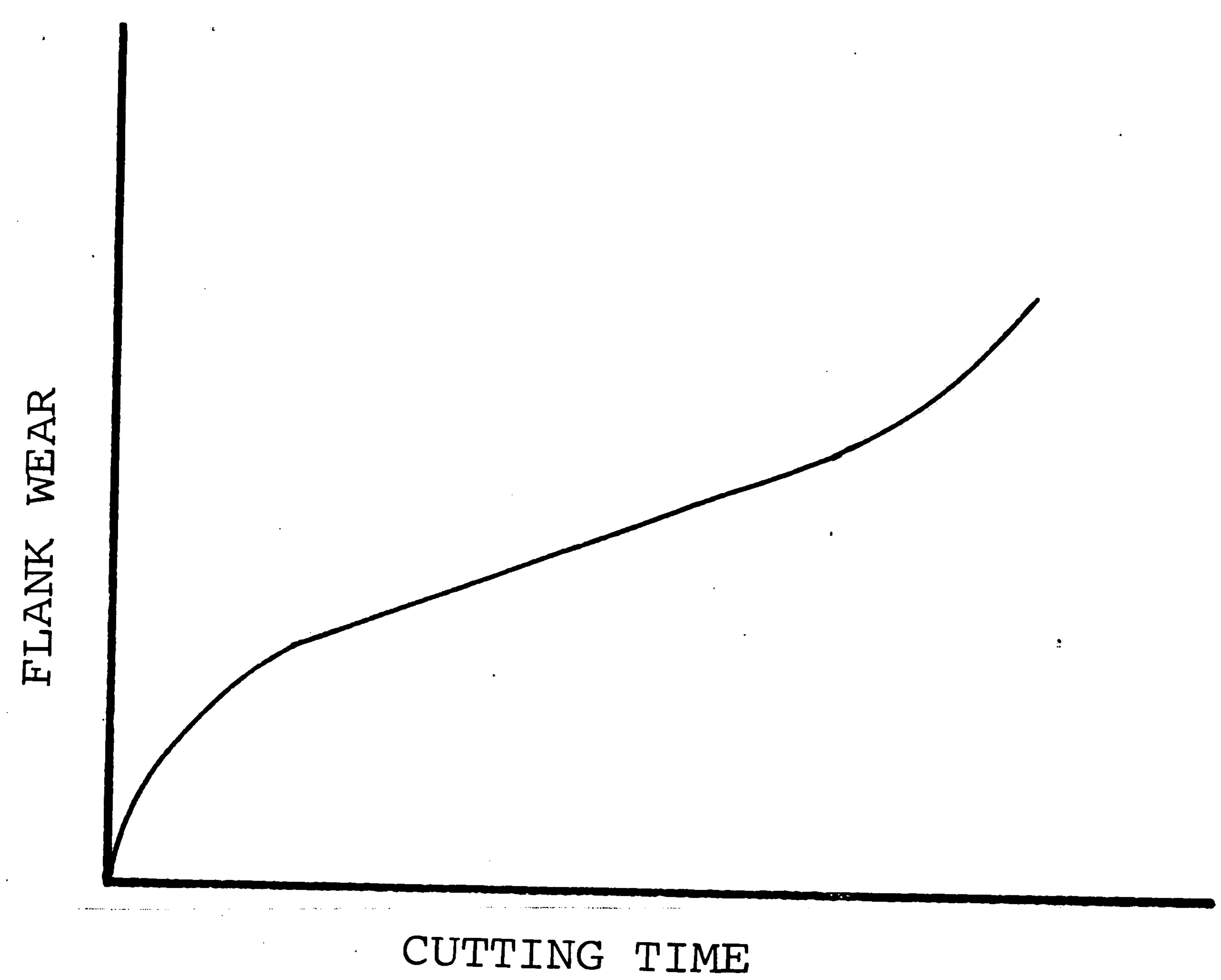

Fig. 3 - Development of Flank Wear for Carbide Cutting Tools.

thesis is to show how deformation varies as the general wear curve is traversed.

Trent also points out that at the beginning of a cut the apparent wear is due to the deformation of the tip, since the original grinding marks can still be seen on the flank of the tool. The flank has not been worn away, and the wear is the distance between the original face of the tool and the deformed face.

Trent's comment concerning the grinding marks still being found on the flank of the tool is quite interesting. Vieregge listed five different mechanisms of wear, two of them being abrasion and deformation. From a purely theoretical standpoint, abrasion should never occur between the flank of the tool and the workpiece. Trent says that before there is any abrasion, the tip of the tool is deformed, creating the bulge on the flank of the tool. As this bulge increases, the flank is forced against the workpiece. When it comes in contact, abrasion results. This abrasion goes into the make-up of what is termed flank wear.

The development of deformation during a cut was the first consideration in this experimental work. Since the deformed portion of the tool comes in contact with the workpiece and abrasion results, no true deformation rate can be found by studying just the deformation on the flank of the tool. To get a true estimate of how deformation varies with cutting time, the faces of certain tools were ground down to provide a step at the tool tip .050 inches long and .030 inches higher than the rest of the face of the tool. Such a tool is shown in Fig. 4.

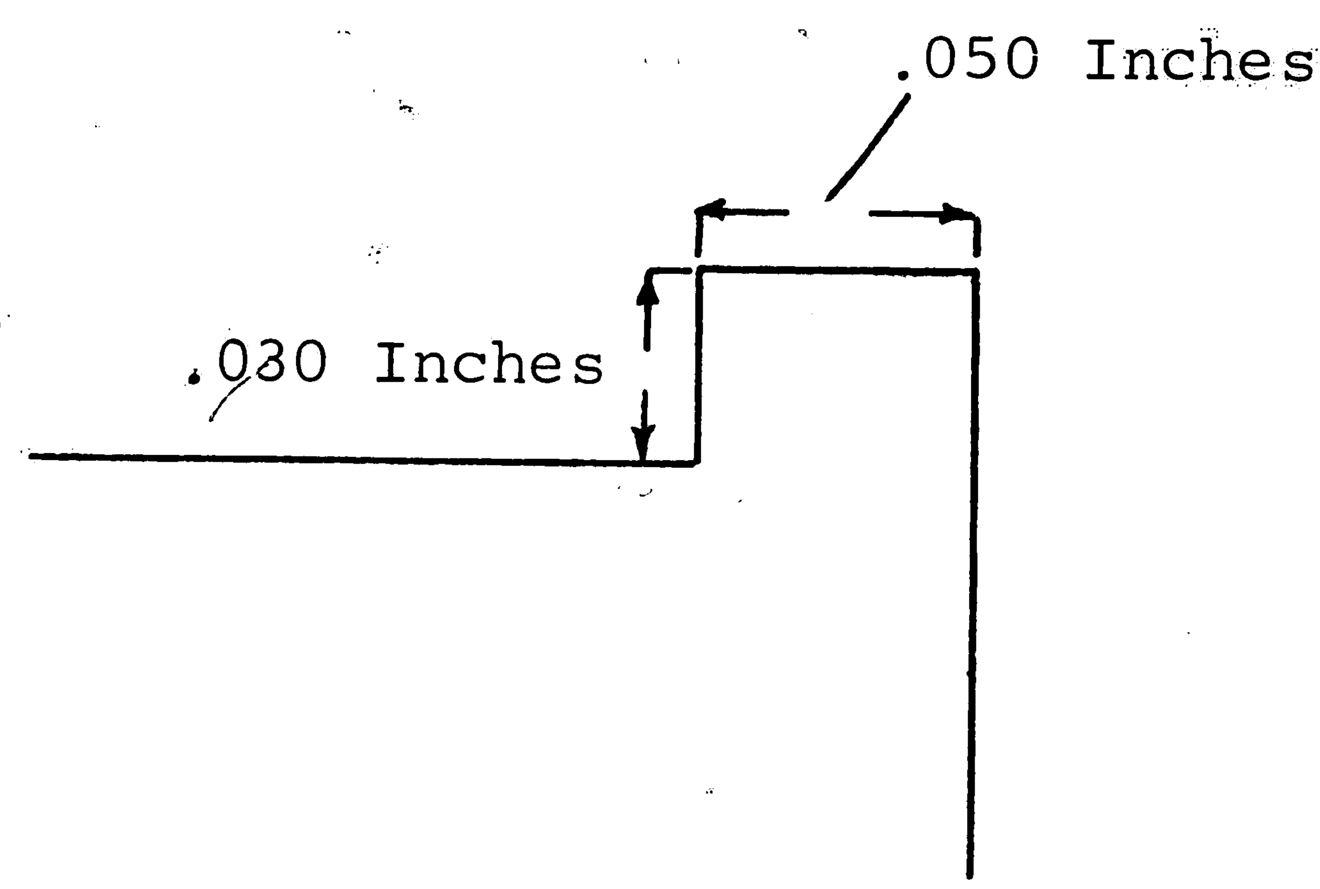

Fig. 4 - Step Tool Used in Experimental Work.

The cutting or compressive force that is present should compress the tool material, and deformation should be visible at the rear of the step. The radial force may also compress the tool material, and additional deformation would be produced.

Abrasion occurs between the underside of the chip and the face of the tool. This abrasion process partially accounts for the crater on the face of the tool. Part of the deformation at the rear of the step should be worn away. However, it is doubtful whether any significant portion of the deformation is worn away, since the depth of the crater is not very large when compared to the .030 inch step. Two different rates of deformation were studied with the step tools.

The next consideration in this experimental work was a further investigation of the process of flank deformation with varying wear rates. To change the rate of wear, the feeds and speeds were varied. Step tools were not used since the previous study has produced the behavior of true deformation in cemented carbides.

Selection of Conditions

One standard commercial grade of carbide was used to examine the relationships that exist between deformation and wear. This carbide has a structure of tungsten, titanium, and tantalum carbide grains and cobalt. Both the existing temperatures and pressures must be of sufficient magnitude in order to produce deformation. The grade of carbide selected is capable of cutting at conditions of high temperature and pressure.

In order to study deformation, the tool must be capable of deforming. A hard, brittle tool will chip and break before there is any noticeable deformation. The carbide selected has an 8 per cent cobalt composition. This composition was chosen since higher percentage cobalt compositions are less resistant to deformation. To go any higher in cobalt composition would result in a sacrifice of hardness. The tool would thus tend to crumble under the conditions of high temperatures and pressures.

The conditions under which deformation take place also influence the selection of a work material. The heat associated with the plastic deformation of the chip is the primary contributor to the heat generated in a metal cutting operation. The amount of heat generated will increase as the shear strength of the work material is increased. 4340 steel, which has a fairly high shear strength, was chosen.

Appendix A contains a brief outline of the compositions and properties of both tool and work material used in this experimental work.

In selecting the actual cutting conditions, attention must be given to the general wear curve. In studying how deformation is related to wear, deformation must be examined over the entire wear curve. The cutting conditions that have been selected insure this.

Appendix B contains an outline of the cutting conditions used in this experimental work.

Experimental Procedure

In the study of the development of deformation, five different cutting conditions were used. These conditions were different only with respect to cutting time. The speed, feed, and depth remained constant. At each condition three cuts were made. Two sets of cuts were made to insure that the mechanisms of cutting were not changed due to the creation of the step. With both the regular and the step tools, a total of thirty cuts was made. These thirty cuts were taken in random order.

The flank wear and the deformation on the step of the tool were measured with a tool maker's microscope. To aid in the measurement of deformation on the flank of the tool, a special fixture was made and attached to a tool maker's microscope. It allows the tool to be rotated while the analyst looks through the microscope and measures deformation. This fixture makes possible the easy location of the point of maximum deformation on the flank of the tool.

To further aid in the study of the development of deformation, the feed was lowered and a series of cuts were taken. There were seven conditions. Only the cutting times differed. Three cuts were made at the lower cutting times, while only two cuts were taken at the two highest cutting times. A total of nineteen cuts was the result. The deformation and wear were measured in the same manner as above.

In the investigation of the process of deformation with changing wear rates, the speeds and feeds were varied. First, the feed was changed in increments of .010 inches per revolution, from .010 to .050 inches per revolution while speed, depth of cut, and cutting time remained constant. Two cuts were made at each condition. Then the cutting speed was changed in increments of 50 surface feet per minute, from 300 to 600 surface feet per minute. Here the feed rate was constant with depth of cut and cutting again time remaining the same. Two cuts were taken at each condition. Since there was no step, only flank wear and deformation were measured. As in all other cases, the cuts were taken in random order.

Results

The graphs of deformation as related to the various variables are found in Appendix C. The statistical analyses for the calculated equations are given in Appendix D. The developed third order equations are found in the results and also in Appendix D. The first and second order equations are given in Appendix D.

From graph 1, it can be seen that the deformation at the rear of the step of the tool increased as the duration of a cut was lengthened. When the feed was decreased to .015 inches per revolution, deformation was not seen on the rear step until the cutting time had been increased to 240 seconds. For times of cutting longer than 240 seconds, the deformation at the rear of the step increassed.

Equations of the third order showing deformation as a function of time were obtained using the method of least-squares. The method of least-squares is a technique for estimating a function that minimizes the sum of the squares of the deviations from the estimate. Checking the statistical analyses, all the F-values are seen to be significant. What this means is that the mean square, which is based on the sum of the squares of the deviations between the observed and the calculated values, the residual, divided by the number of degrees of freedom, is very small when compared to the sum of the squares of the deviations between the mean and the calculated values divided by its degrees of freedom. This last sum is called regression in Appendix D. The total sum of the squares, the regression plus the residual, is equal to the sum of the squares of the deviations between the observed values and the mean. As each higher order equation is calculated, the goodness of fit should become more exact. However, from our results, it can be seen that for a higher order fit, the F-value showing significance may decrease. For each higher order fit, the regression sum of the squares becomes larger and the number of degrees of freedom also increases. The residual sum of the squares will decrease, and the residual will also lose a degree of freedom. This combination of occurrences may produce a smaller F-value, but as the degrees of freedom change, the significance of any F-value also changes. Thus, the smaller F-value may be more significant.

When the feed rate was equal to .030 inches per revolution, the following third order equation resulted for the deformation at the step:

$$sd = -.30423 + .63177\ t - (3.16871 \times 10^{-3})\ t^2 + (1.82897 \times 10^{-3})\ t^3$$

where sd = deformation at the rear of the step of the tool $\times 10^{-4}$ (inches)

t = cutting time (seconds)

For these same cuts, the deformation on the flank of the tool increased when the cutting time was lengthened from 15 to 30 and then to 45 seconds. When the cutting time was increased beyond 45 seconds, the flank deformation seemed to remain fairly constant. This trend is observed at both feed rates below 75 seconds. With the feed rate at .015 inches per revolution, there was an increase in flank deformation as the cutting time was increased from 75 seconds to 240 seconds. This increase was not very large.

Equations for flank deformation as a function of time were calculated for both feed rates. The following were the results:

feed rate = .030 inches per revolution

$$fd = -.02909 + 1.00314\ t - .01154\ t^2 + (3.10922 \times 10^{-5})\ t^3$$

feed rate = .015 inches per revolution

$$fd = 1.58439 + .21932\ t - (9.42532 \times 10^{-4})\ t^2 + (1.42344 \times 10^{-6})\ t^3$$

where fd = deformation on the flank of the tool x 10^{-4} (inches)

The flank wear on the step tools increased sharply as the cutting time was increased to 45 seconds. After 45 seconds the increase in flank wear was at a much slower rate. Equations for flank wear as a function of cutting time for both feed rates follow:

feed rate = .030 inches per revolution

$$w = -.80692 + 9.03664\ t - .13161\ t^2 + (6.34663 \times 10^{-4})\ t^3$$

feed rate = .015 inches per revolution

$$w = 9.56998 + 1.39795t - (8.17506 \times 10^{-3})t^2 + (1.85413 \times 10^{-5})t^3$$

where w = flank wear x 10^{-4} (inches)

Functions were then developed to express both flank and face deformation as a function of flank wear. As flank wear increases, the deformation at the rear of the step increased at a very steady rate. The deformation on the flank of the tool increased at first, but as the flank wear further increased, the flank deformation remained fairly constant. The flank deformation started to decrease at the higher values of flank wear. Equations for flank and face deformation as a function of flank wear were not developed for the data taken with the feed rate equal to .015 inches per revolution. This was due to the fact that no deformation was seen at the rear of the step of the tool for short cutting times. The developed equations are:

$$sd = .14608 - .02831\ t + (1.31442 \times 10^{-3})t^2 - (2.41032 \times 10^{-6})t^3$$

$$fd = .02428 + .05336\ t + (1.7295 \times 10^{-3})t^2 - (4.12946 \times 10^{-6})t^3$$

When the same series of cuts were made on regular tools without any step, the results were practically the same. Trigger and Chao (6) have shown that as the length of natural chip contact is decreased, the interface temperature decreases. The minimum interface temperature occurs when the chip contact length is one-third the natural contact length. In most of the cuts with the step tools, the chip contact length has been decreased. However, the results show no significant difference in either wear or deformation. The curves for these cuts are found in Appendix C but no statistical analysis has been performed on the data.

Graphs 8 - 11 illustrate the relationships between both flank wear and flank deformation and increases in the feed rate and the cutting speed. There was a small increase in flank wear as the feed rate was changed from .010 to .020 inches per revolution. However, the flank deformation, of which there was none at a feed rate of .010 inches per revolution, increased sharply when the feed rate was changed to .020. The flank wear increased sharply when the feed rate was changed to .030 inches per revolution, remained practically the same at .040, and then rose again at a feed rate of .050. There was very little difference in the flank deformation with increases beyond .020 inches per revolution. The equations for flank wear and flank deformation as a function of feed rate are:

$$w = -3.80949 + .76348 f + .25333 f^2 - (6.11118 \times 10^{-4})f^3$$

where f = feed rate x 10^{-3} (inches per revolution)

$$fd = -1.60714 + .68988 f + (3.39290 \times 10^{-3})f^2 - (1.66667 \times 10^{-4})f^3$$

Graphs 10 and 11 illustrate flank wear and deformation as a function of cutting speed. As the cutting speed is increased, the amount of flank wear and flank deformation also increase. When the cutting speed was increased from 550 to 600 surface feet per minute, the flank wear decreased. The equations for flank wear and flank deformation as a function of cutting speed are:

$$w = (5.88150 \times 10^2) - 4.06304 V + (9.00619 \times 10^{-3})V^2 - (5.6720 \times 10^{-6})V^3$$

where V = cutting speed (surface feet per minute)

$$fd = 45.64070 - .43717V + (1.25320 \times 10^{-3})V^2 - (9.98850 \times 10^{-7})V^3$$

The final graphs, 12 and 13, show how flank deformation varied as flank wear increased due to increasing feed rates and cutting speeds. In both cases, the deformation increased with increases in the lower feeds and speeds. However, above a certain feed rate, .020 inches per revolution, and above a certain cutting speed, 500 feet per minute, the flank deformations remained fairly steady for any subsequent increases in flank wear. The equations are:

Varying the feed rate,

$$fd = -1.41544 + .26788W - (9.32462 \times 10^{-4})W^2 + (9.08426 \times 10^{-7})W^3$$

Varying the cutting speed,

$$fd = -4.41835 + .27762W - (4.70020 \times 10^{-4})W^2 + (2.32161 \times 10^{-6})W^3$$

Discussion

It appears from the results that the deformation at the rear of the step, the so-called true deformation, definitely increases with increased cutting times. This deformation was not the only visible phenomena at the rear of the step. An oxide layer was also seen. This oxide layer was particularly evident for the cuts at the longer cutting times. For the cuts at .015 inches per revolution and 280 seconds, the oxide layer reached a magnitude of about .004 inches.

Another interesting observation concerning the step tools was that no deformation was visible at the rear of the step unless the crater extended the whole length of the step. The crater would thus be about .050 inches long. When the feed was reduced from .030 to .015 inches per revolution, the crater did not reach the end of the step until 240 seconds of cutting had passed. No deformation was visible up to that time. If the crater area is the area over which the cutting force is applied, the deformation at the flank of the tool may be the result of the downward force compressing the carbide tool material and creating the bulge on the flank of the tool. The distance between the flank of the tool and the beginning of the crater is not great and under these particular conditions was practically negligible. When the crater did reach the end of the step, deformation also resulted. Deformation was now visible at both ends of the crater. Trent concludes in his article that the cratering type of wear in alloys containing free tungsten carbide is due to the formation of a fused alloy between the chip and the tool. There is no doubt that diffusion does take place between the carbide tool and the steel chip. However, the previous observations may indicate that the crater may be partially caused by a displacement of tool material. The compressive force pushes down on the top of the tool compacting the tool material and creating the crater. This displacement creates the bulge that was found on both sides of the crater with the step tool, but is usually just seen on the flank of the tool.

Conclusions

(1) The deformation at the rear of the step increases with increasing flank wear.

The equations shown in the results for step deformation as a function of cutting time and flank wear are third order equation. However, the graphs of step deformation as a function of cutting time and flank wear show that straight lines or linear equations will also closely approximate the actual relationships. Both the first and third order equations provide excellent statistical models. The F-values of both types of equations are extremely significant.

(2) The deformation on the flank of the tool increases up to a certain point, about .020 inches, with increasing flank wear. After this point has been reached, the flank deformation remains fairly steady and then decreases.

The flank deformation should behave much in the same fashion as the deformation at the rear of the step. The compressive force should compress the tool material and cause deformation on both sides of the crater. The only difference is that the radial force component may cause greater deformation at the rear of the step. But as the tool material bulges on the flank, the interference between the workpiece and the tool prevents the flank deformation from increasing in the same manner as the step deformation increases. Trent pointed out he saw deformation on the flank before any abrasion wear was visible. If there is this deformation on the flank of the tool, it is very easy to see why mechanical interference occurs between the tool and the workpiece. The workpiece will grind down the flank deformation, abrasion wear will be visible, and the flank deformation will be seen further down on the flank of the tool. As the flank wear further increases, it becomes more difficult for deformation to occur since the temperature decreases as the distance between the bottom of the flank wear and the tool-chip interface increases.

(3) For changes in speeds or feeds, flank deformation increases for just the smaller values of flank wear. With further increases in flank wear, there were no subsequent increases in flank deformation. The transition point is at about .020 inches flank wear.

Schwartzkopf and Kieffer (7) point out that as feed or speed is increased, the temperatures in cutting are also increased. Trigger and Chao (8) have developed equations showing the interface temperature as an exponential function of first the speed, and then the feed rate. With increasing feed rates, the pressure exerted on the tool also increases. Increases in temperature and pressure should increase the rate of flank wear. Trent concluded that at high temperatures and pressures, the rate of deformation is increased. However, past that certain transition point, there were no increases in flank deformation. The interference between the tool and the workpiece again prevented any increase in flank deformation despite the presence of higher temperatures and pressures.

Areas for Future Consideration

(1) The deformation on the rear of the step raises a question concerning the development of crater wear. Diffusion has been accepted by Trigger and Chao (9) and Trent as the cause of crater wear. If material is found on the rear of the step, displacement must have occurred. An investigation of the role of compression in causing the crater should be conducted.

(2) Further work on the role of the oxide coating in cutting with carbides should be considered. In this work, the oxide was seen to form on the rear of the step. This oxide must have also formed on the flank of the tool but was wiped away. Did this oxide layer aid or hinder the development of flank wear and deformation?

(3) The relationships between flank wear and deformation have been investigated here. It has been shown that flank deformation is a cause of flank wear. Further work should be conducted to see to what extent deformation causes flank wear.

(4) When the temperature is increased, the rate of deformation also increases. Trent arrived at this conclusion, and it is generally accepted as true. However, due to the inability of experimenters to actually measure the temperatures in metal cutting, no one has shown the

development of deformation with changes in temperature. This certainly is an area for future investigation.

Appendix A

1. Tool Material

The cemented carbides used in these tests were manufactured by Metallurgical Products Department of the General Electric Company. Grade 370 was the particular grade used. The chemical composition of this grade is 72 percent tungsten carbide, 8 percent titanium carbide, 11.5 percent tantalum carbide, and 8.5 percent cobalt. It has a Rockwell A hardness of 91.1.

2. Work Material

AISI - 4340 steel was used in the testing as the work material. The chemical composition is as follows:

C	Mn	P	S	Si	Ni	Cr	Mo
.40	.68	.020	.013	.28	1.87	.74	.25

The above figures are percentages. The Brinell Hardness Number is 303.

Appendix B

Cutting Conditions

All cuts were made on a LeBlond engine lathe. The carbide inserts were triangular, and the nose radius was a sixteenth of an inch. The side cutting edge angle was 0 degrees, and the effective back rake angle was -8 degrees. The following cutting conditions were used for the measurements indicated.

<u>Measurements of deformation on the step and the flank and the flank wear for changes in cutting time for both tools with and without a step.</u>

Cutting Speed = 500 surface feet per minute

Feed Rate = .030 inches per revolution for first set of cuts and .015 inches per revolution for second set

Depth of Cut = .040 inches

<u>Measurements of deformation on the flank and the flank wear for changes in feed rate.</u>

Cutting Speed = 500 surface feet per minute

Depth of Cut = .050 inches

Cutting Time = 30 seconds

<u>Measurements of deformation on the flank and the flank wear for changes in cutting speed.</u>

Feed Rate = .040 inches per revolution

Depth of Cut = .050 inches

Cutting Time = 30 seconds

APPENDIX C

GRAPH 1. DEFORMATION AT THE STEP OF THE TOOL
vs. CUTTING TIME

a. Feed Rate = .030 Inches Per Revolution
b. Feed Rate = .015 Inches Per Revolution

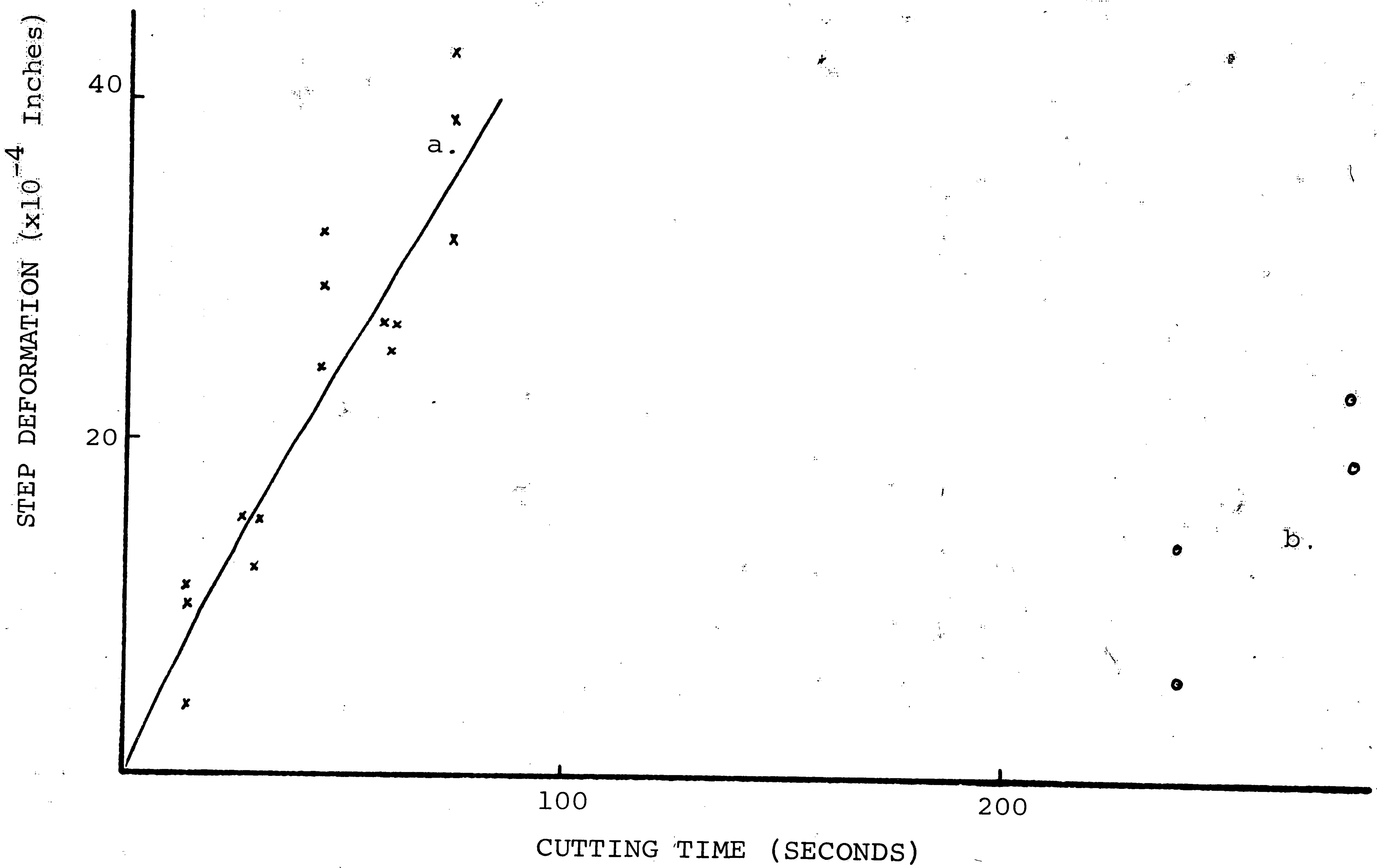

GRAPH 2. FLANK DEFORMATION vs. CUTTING TIME (STEP TOOLS)

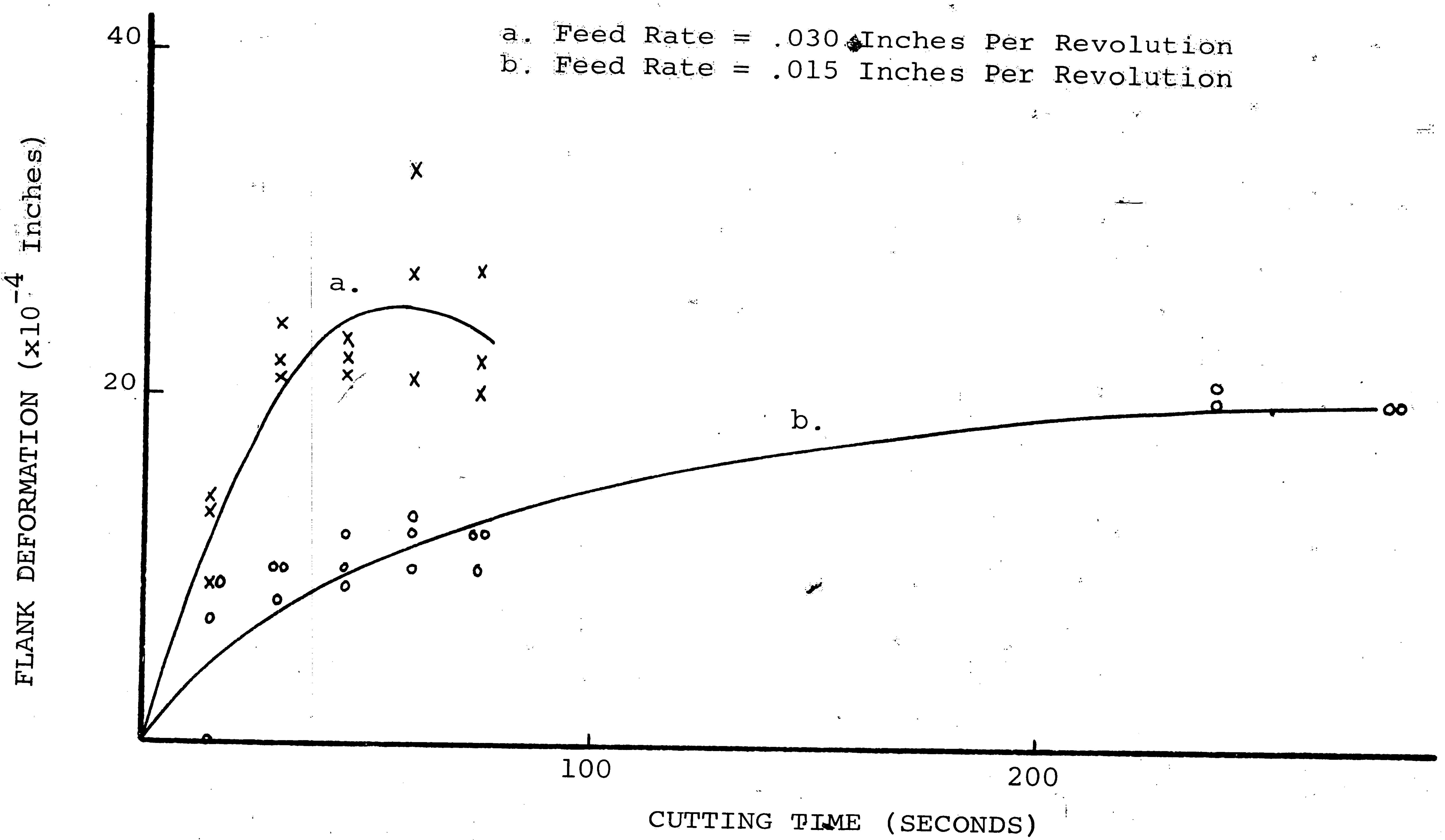

GRAPH 3. FLANK WEAR vs. CUTTING TIME (STEP TOOLS)

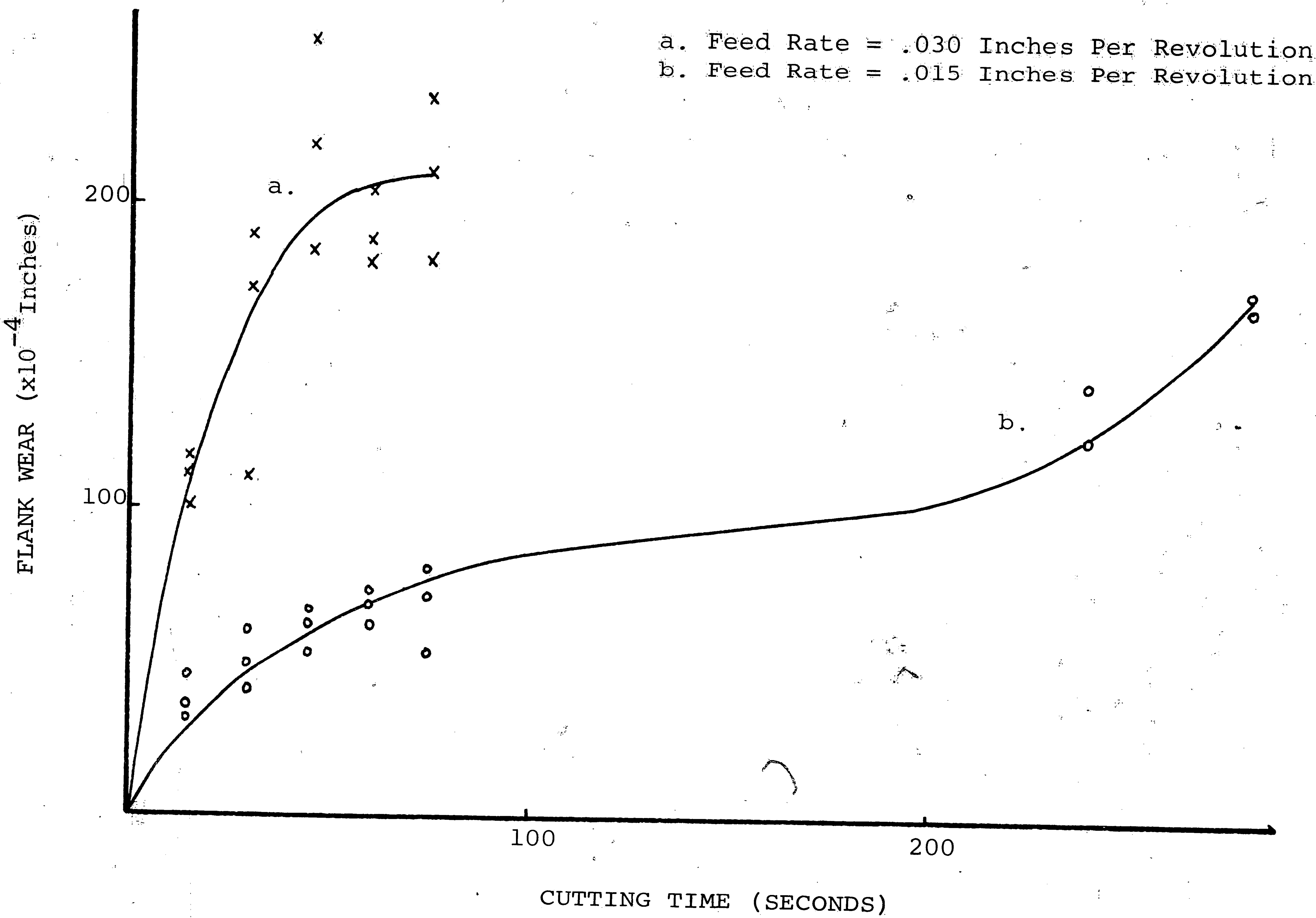

GRAPH 4. DEFORMATION AT THE STEP OF THE TOOL vs. FLANK WEAR

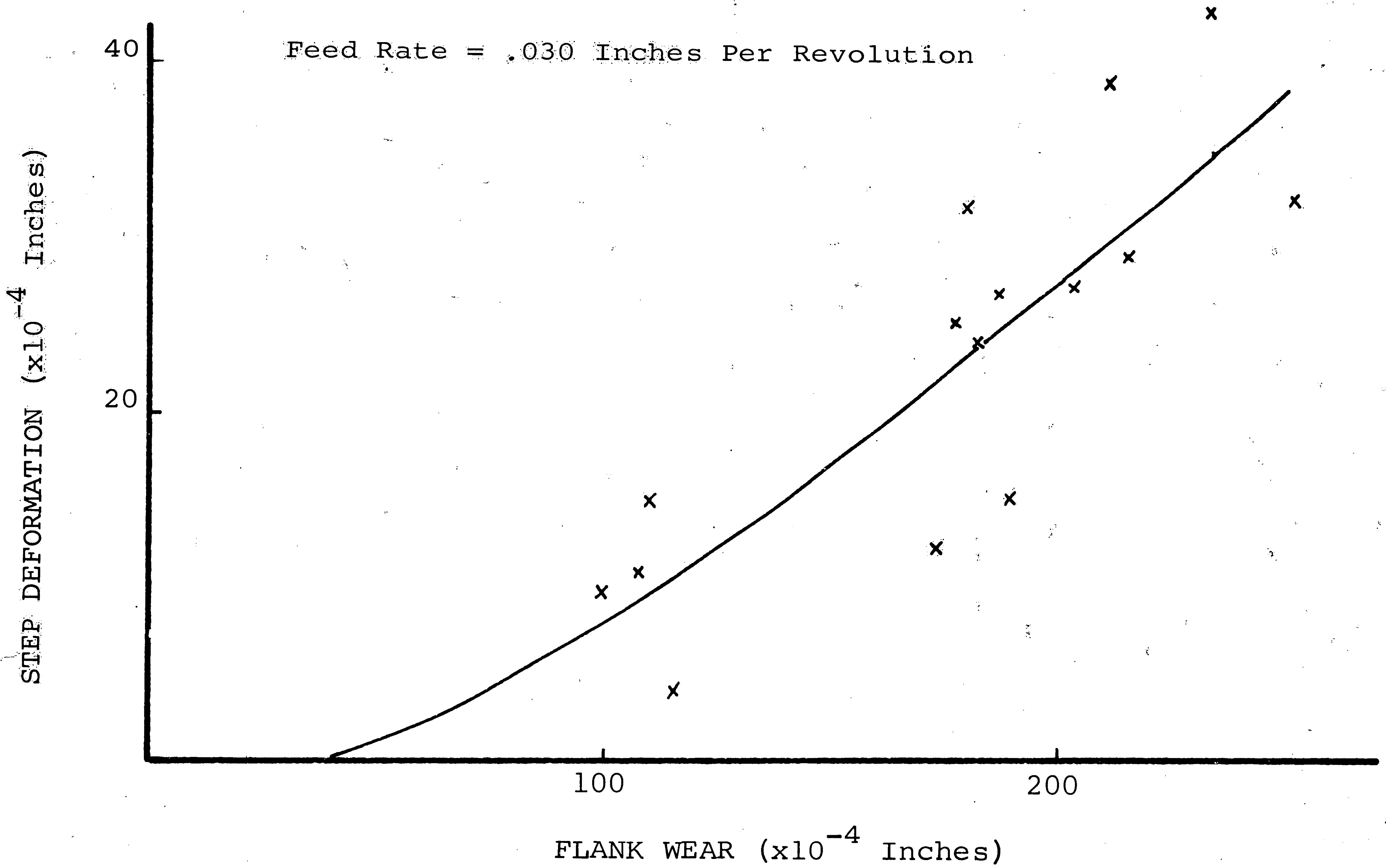

GRAPH 5. FLANK DEFORMATION vs. FLANK WEAR (STEP TOOLS)

Feed Rate = .030 Inches Per Revolution

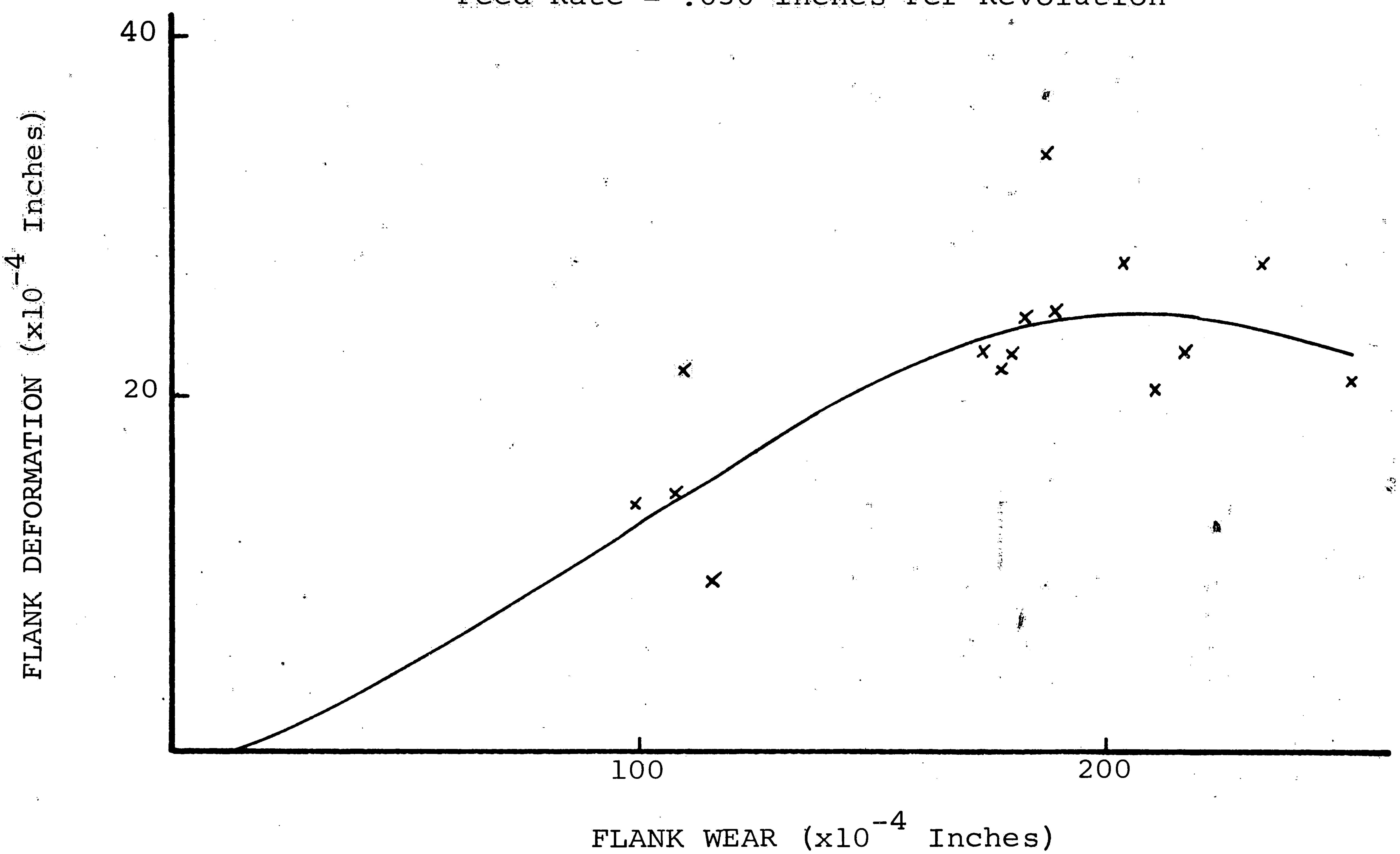

GRAPH 6. FLANK DEFORMATION
vs. CUTTING TIME (NON-STEP TOOLS)

a. Feed Rate = .030 Inches Per Revolution
b. Feed Rate = .015 Inches Per Revolution

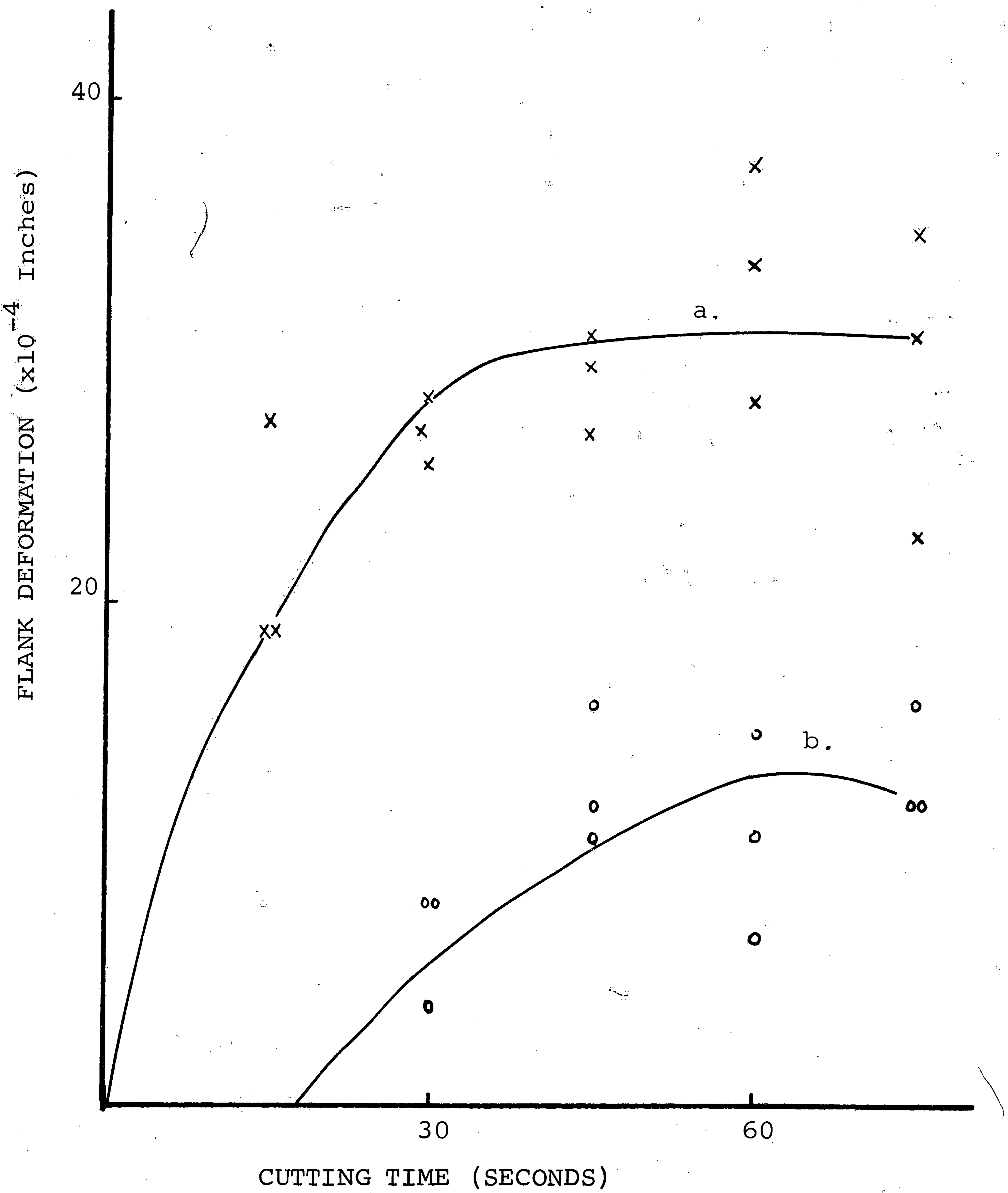

GRAPH 7. FLANK WEAR vs. CUTTING TIME
(NON-STEP TOOLS)

a. Feed Rate = .030 Inches Per Revolution
b. Feed Rate = .015 Inches Per Revolution

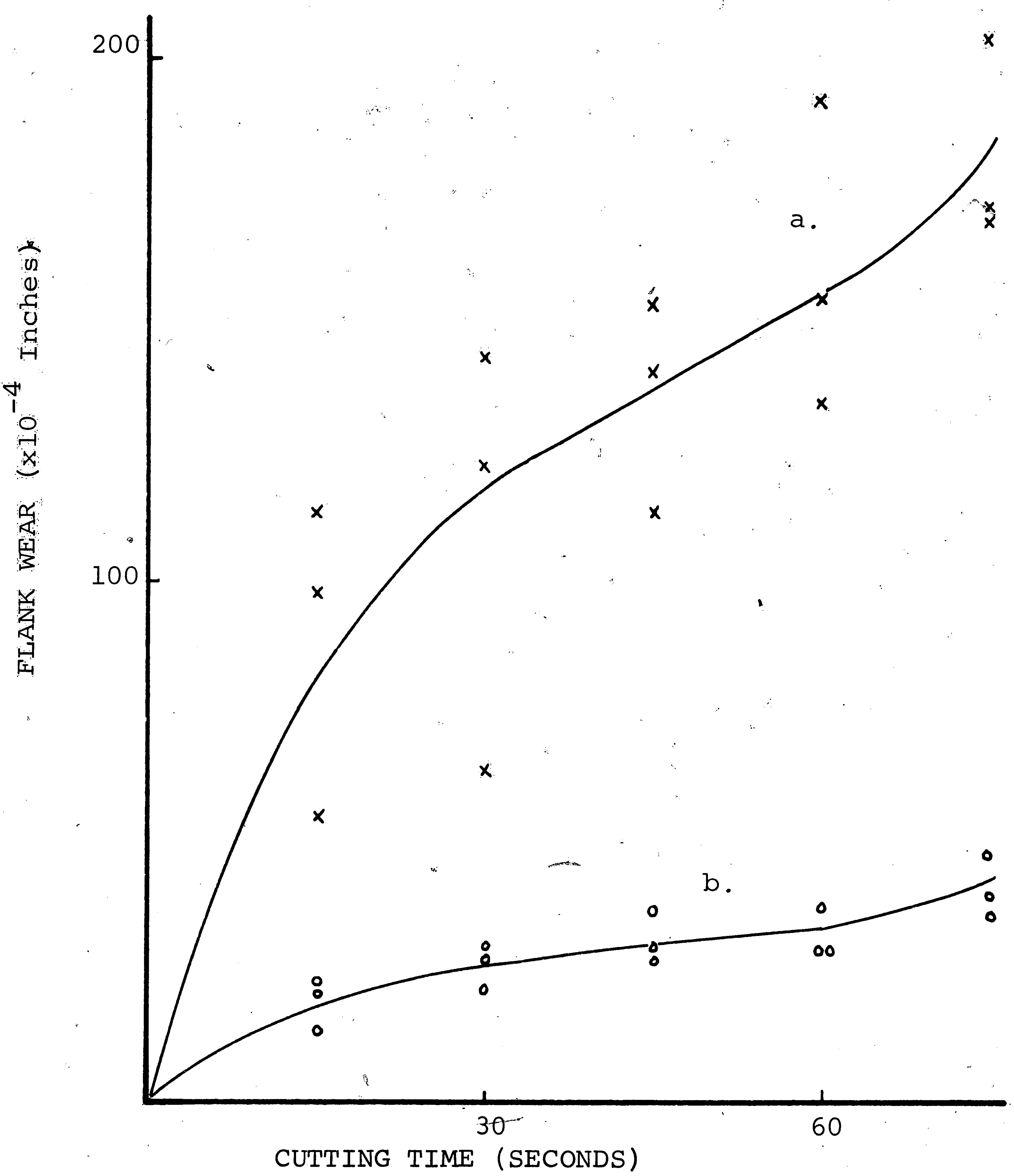

GRAPH 8. FLANK WEAR vs. FEED RATE

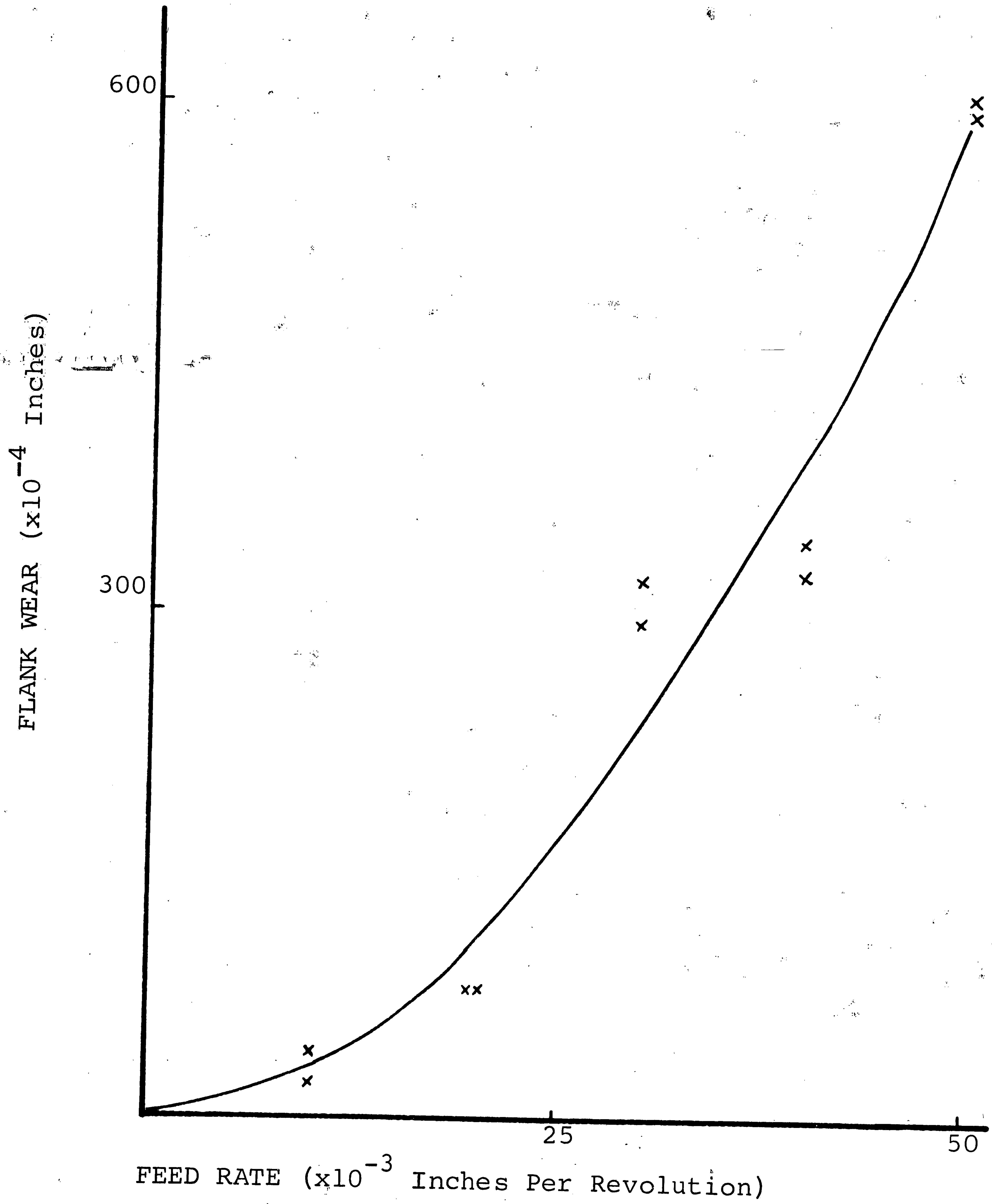

GRAPH 9. FLANK DEFORMATION vs. FEED RATE

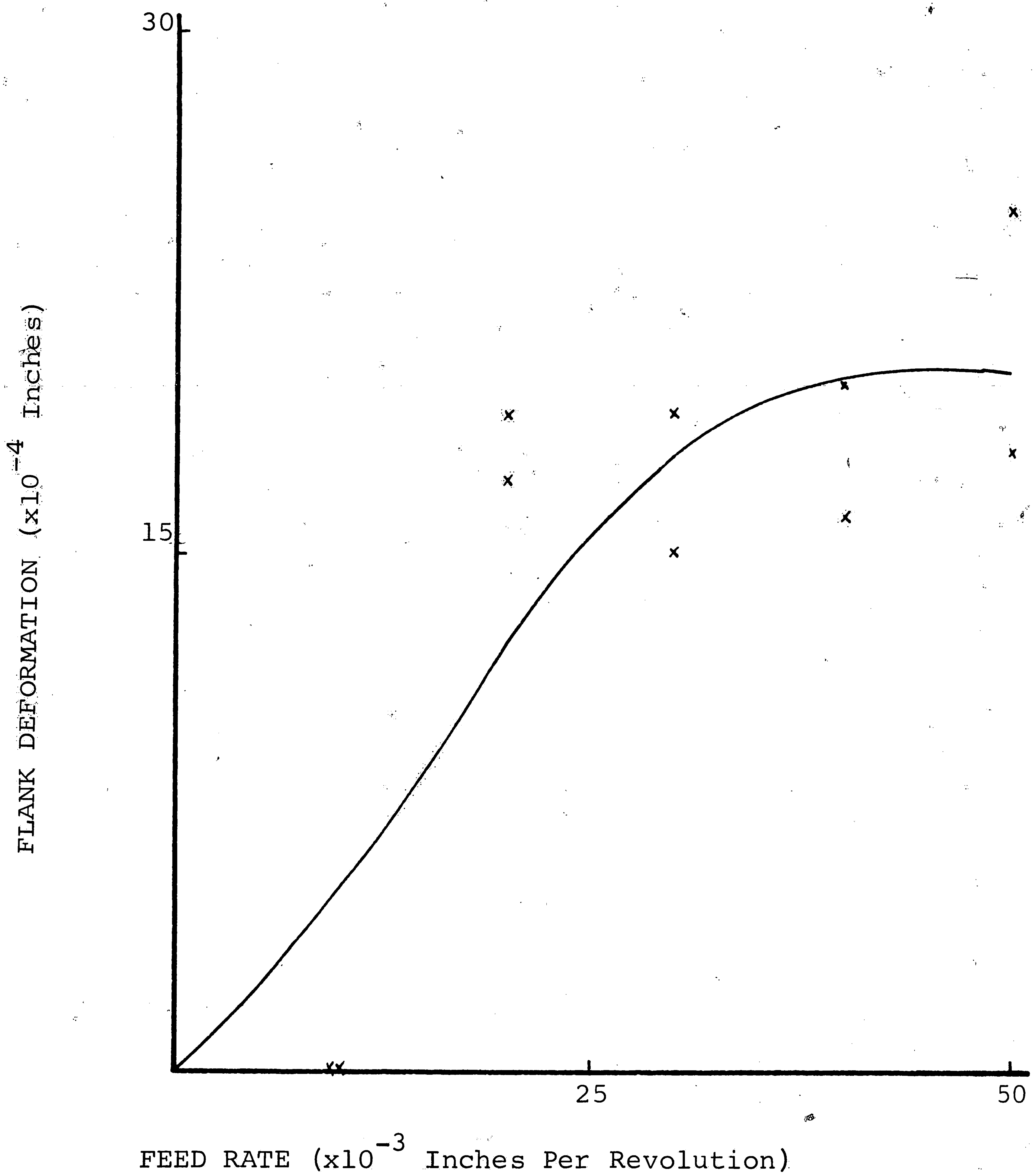

GRAPH 10. FLANK WEAR vs. CUTTING SPEED

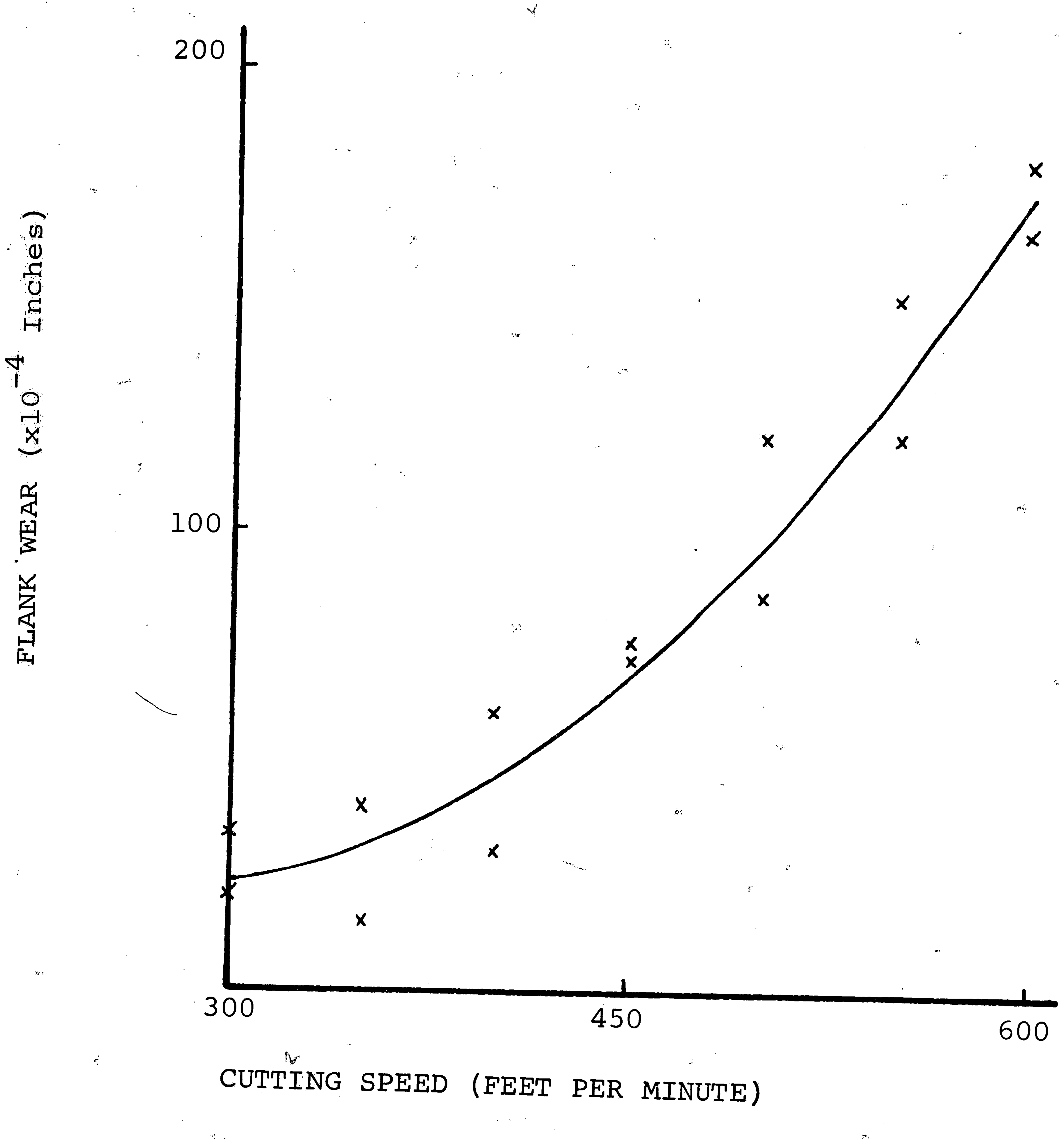

GRAPH 11. FLANK DEFORMATION vs. CUTTING SPEED

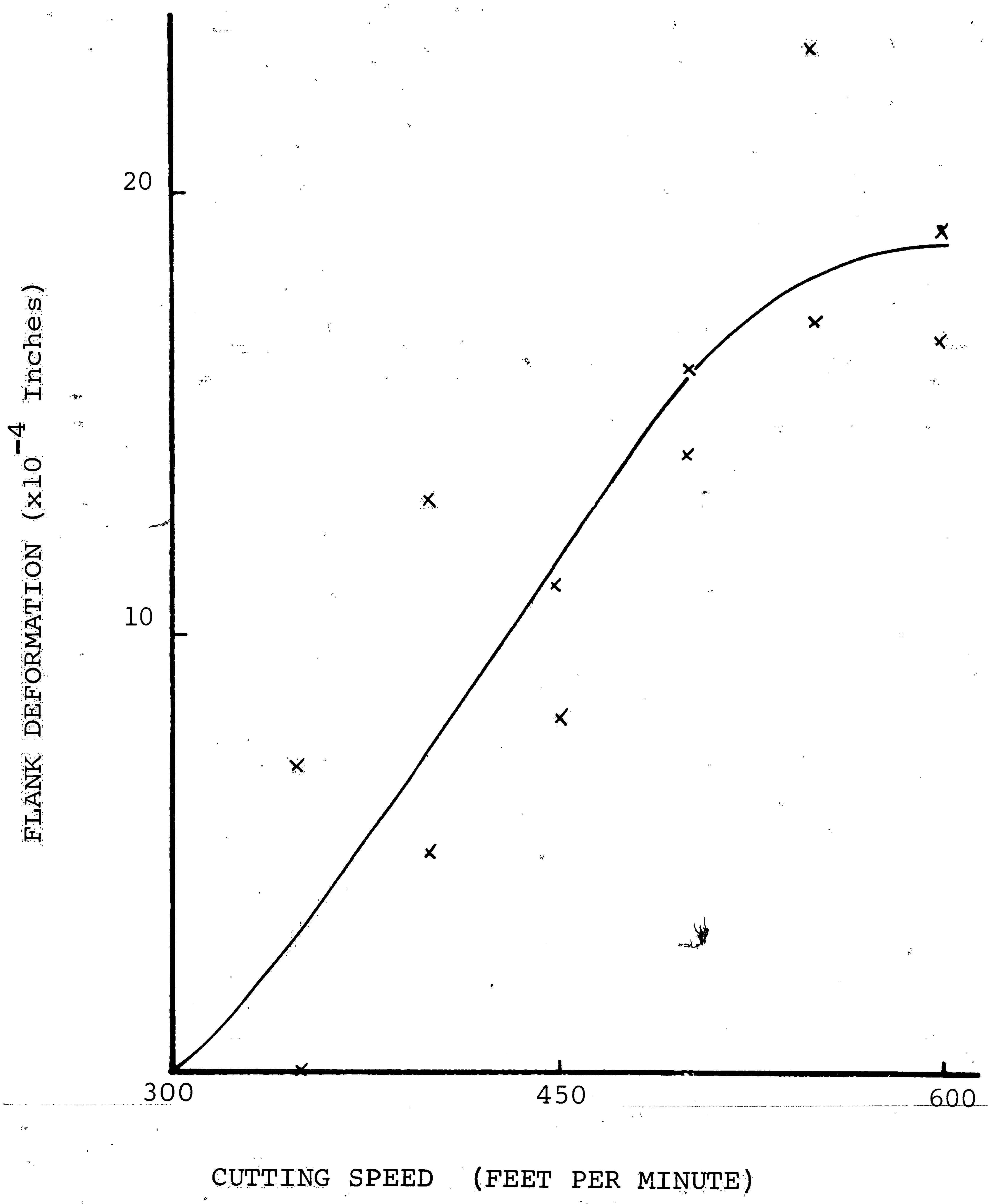

GRAPH 12. FLANK DEFORMATION vs. FLANK WEAR (VARYING FEED RATES)

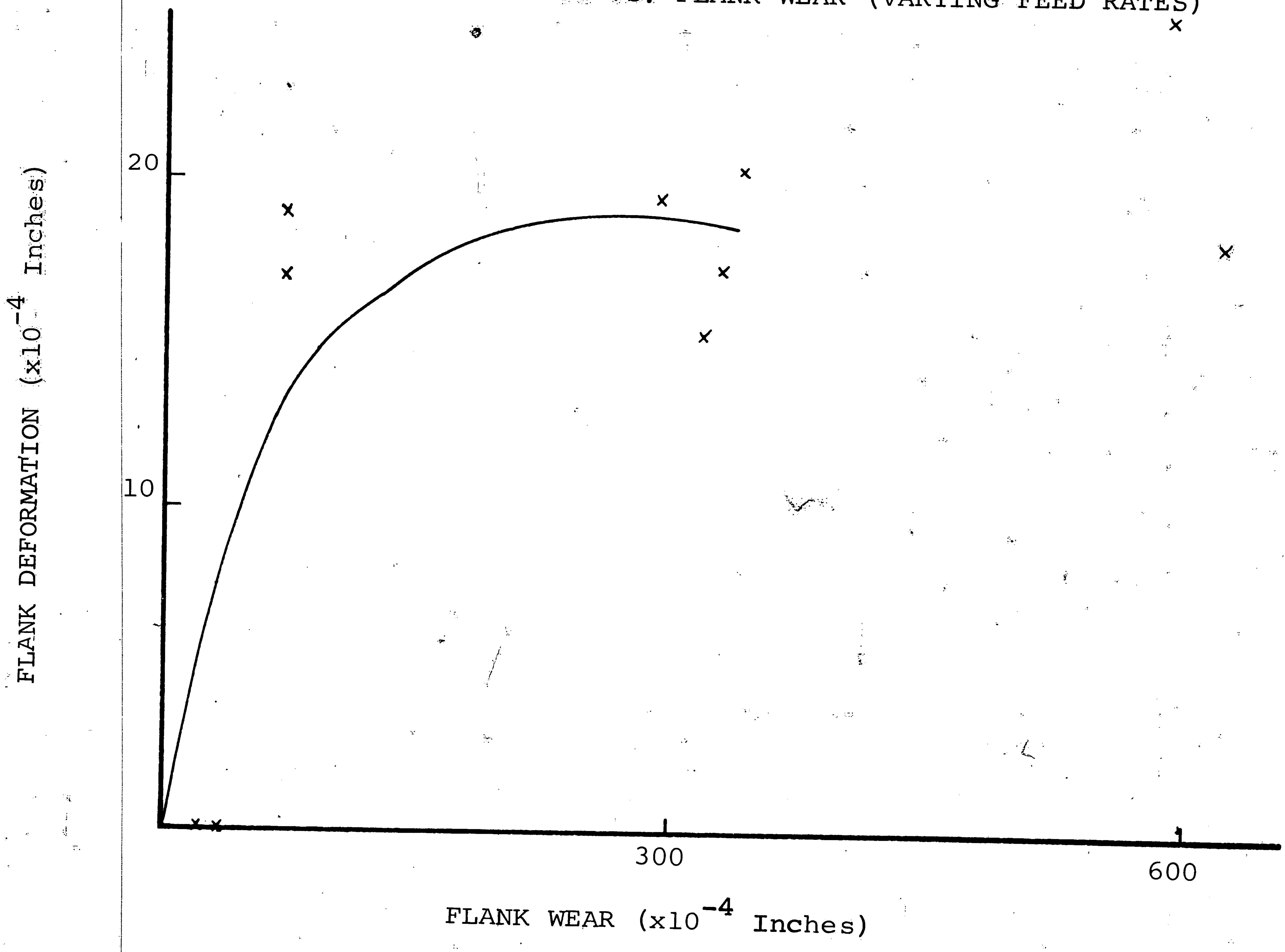

GRAPH 13. FLANK DEFORMATION vs. FLANK WEAR
(VARYING CUTTING SPEEDS)

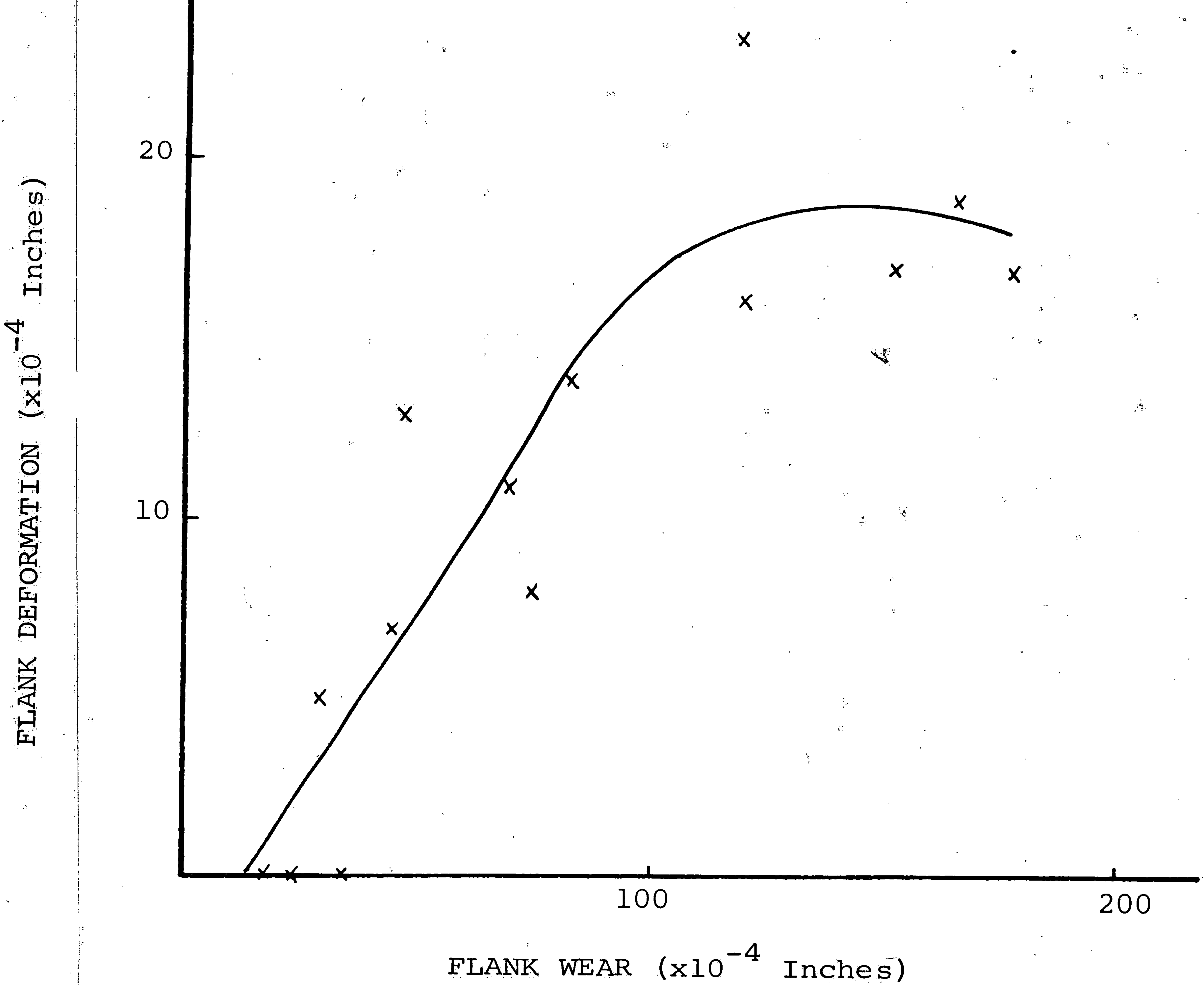

Appendix D

Statistical Analyses

1. Deformation at the step as a function of cutting time

(f = .030 /rev)

Third order equation

$$sd = -.30422 + .63177t - (3.16869 \times 10^{-3})t^2 + (1.82896 \times 10^{-5})t^3$$

Analysis of Variance

	Sum of Squares	Degrees of Freedom	Mean Square	F
Regression	9480.3597	4	2370.0899	123.51557
Residual	268.64029	14	19.188592	

Second order equation

$$sd = -.11904 + .57539t - (1.11111 \times 10^{-3})t^2$$

	Sum of Squares	Degrees of Freedom	Mean Square	F
Regression	9479.6190	3	3159.8730	175.95190
Residual	269.38098	15	17.958732	

First order equation

$$sd = .71428 + .49206t$$

	Sum of Squares	Degrees of Freedom	Mean Square	F
Regression	9472.6190	2	4736.3095	274.19018
Residual	276.38098	16	17.273811	

2. Flank deformation as a function of cutting time

(f = .030 /rev)

Third order equation

$$fd = -.02909 + 1.00314t - .01154t^2 + (3.10922 \times 10^{-5})t^3$$

Regression	7114.8358	4	1778.7090	157.44355
Residual	158.16415	14	11.297440	

Second order equation

$$fd = .28571 + .90730t - (8.04232 \times 10^{-3})t^2$$

Regression	7112.6952	3	2370.8984	221.84905
Residual	160.30484	15	10.686989	

First order equation

$$fd = 6.31746 + .30412t$$

Regression	6745.9651	2	3372.9825	102.39875
Residual	527.03494	16	32.939684	

3. Flank wear as a function of cutting time (f = .030 /rev)

Third order equation

$$w = -.80678 + 9.03663t - .13160t^2 + (6.34651 \times 10^{-4})t^3$$

Regression	487799.64	4	121949.91	165.28606
Residual	10329.357	14	737.81124	

Second order equation

$$w = 5.61905 + 7.08031t - .06021t^2$$

Regression	486907.74	3	162302.58	216.95770
Residual	11221.260	15	748.08398	

First order equation

$$w = 50.77777 + 2.56444t$$

Regression	466351.49	2	233175.74	117.40415
Residual	31777.512	16	1986.0945	

4. Deformation at the step as a function of flank wear

(f = .030 /rev)

Third order equation

$$sd = .14608 - .028317w + (1.31442 \times 10^{-3})w^2 - (2.41033 \times 10^{-6})w^3$$

Regression	9174.6756	4	2293.6689	55.911545
Residual	574.32440	14	41.023172	

Second order equation

$$sd = - .17815 + .05284w + (4.18417 \times 10^{-4})w^2$$

Regression	9162.8929	3	3054.2976	78.167391
Residual	586.10712	15	39.073808	

First order equation

$$sd = - 2.82670 + .14967w$$

Regression	9064.5905	2	4532.2953	105.85518
Residual	684.40945	16	42.775591	

5. Flank deformation as a function of flank wear

(f = .030 /rev)

Third order equation

$$fd = .02428 + .05336w + (1.17295 \times 10^{-3})w^2 - (4.12947 \times 10^{-6})w^3$$

Regression	7053.0737	4	1763.2684	112.24558
Residual	219.92633	14	15.709024	

Second order equation

$$fd = - .53120 + .19241w - (3.82124 \times 10^{-4})w^2$$

Regression	7018.4893	3	2339.4964	137.88200
Residual	254.51071	15	16.967381	

First order equation

$$fd = 1.76101 + .10862w$$

Regression	6944.8586	2	3472.4293	169.31379
Residual	328.14142	16	20.508839	

6. Flank deformation as a function of feed rate

Third order equation

$$fd = -1.60714 + .68988f + (3.39283 \times 10^{-3})f^2 - (1.66666 \times 10^{-4})f^3$$

Regression	2690.3571	4	672.58928	29.299879
Residual	183.64288	8	22.955360	

Second order equation

$$fd = -2.10714 + .91821f + (-9.10714 \times 10^{-3})f^2$$

Regression	2686.7571	3	895.58570	43.047144
Residual	187.24288	9	20.804765	

First order equation

$$fd = .92857 + .46285f$$

Regression	2624.8286	2	1312.4143	52.671136
Residual	249.17144	10	24.917144	

7. Flank wear as a function of feedrate

Third order equation

$$w = -3.80952 + .76349f + .25333f^2 - (6.11111 \times 10^{-4})f^3$$

Regression	1139411.2	4	284852.80	101.57086
Residual	22435.789	8	2804.4736	

Second order equation

$$w = -5.64285 + 1.60071f + .20750f^2$$

Regression	1139362.8	3	379787.61	152.02191
Residual	22484.184	9	2498.2426	

First order equation

$$w = -74.809 + 11.97571f$$

Regression	1107214.1	2	553607.07	101.33225
Residual	54632.859	10	5463.2859	

8. Flank deformation as a function of cutting speed

Third order equation

$$fd = 45.70180 - .43759V + (1.25416 \times 10^{-3})V^2 - (9.99559 \times 10^{-7})V^3$$

Regression	2241.1988	4	560.28970	52.461925
Residual	106.80121	10	10.680121	

Second order equation

$$fd = -37.51203 + .15214V - (9.52387 \times 10^{-5})V^2$$

Regression	2234.4525	3	744.81749	72.154748
Residual	113.54752	11	10.322501	

First order equation

$$fd = -19.178571 - .06642V$$

Regression	2224.9286	2	1112.4643	108.47011
Residual	123.07143	12	10.255953	

9. Flank wear as a function of cutting speed

Third order equation

$$w = 588.82607 - 4.06778V + (9.01695 \times 10^{-3})V^2 - (5.66509 \times 10^{-6})V^3$$

Regression	131622.29	4	32905.574	162.27988
Residual	2027.7051	10	202.77051	

Second order equation

$$w = 117.20340 - .72536V + (1.36905 \times 10^{-3})V^2$$

Regression	131405.60	3	43801.866	214.67663
Residual	2244.4014	11	204.03648	

First order equation

$$w = - 146.33939 + .50678V$$

Regression	129437.59	2	64718.794	184.36603
Residual	4212.4111	12	351.03426	

10. Flank deformation as a function of flank wear (varying feed rates)

Third order equation

$$fd = - 1.41544 + .26788w - (9.32462 \times 10^{-4})w + (9.08426 \times 10^{-7})w$$

Regression	2667.9129	4	666.97822	25.891116
Residual	206.08713	8	25.760891	

Second order equation

$$fd = 2.74093 + .07849w - (8.12745 \times 10^{-5})w^2$$

Regression	2550.4234	3	850.14112	23.645930
Residual	323.57662	9	35.952958	

First order equation

$$fd = 5.39021 + .03165w$$

Regression	2432.8240	2	1216.4120	27.572037
Residual	441.17597	10	44.117597	

11. Flank deformation as a function of flank wear (varying cutting speed)

Third order equation

$$fd = -4.14183 + .27762w - (4.70020 \times 10^{-4})w^2 - (2.32161 \times 10^{-6})w^3$$

Regression	2237.7019	4	559.42549	50.719432
Residual	110.29806	10	11.029806	

Second order equation

$$fd = -5.38217 + .32876w - (1.12797 \times 10^{-3})w^2$$

Regression	223.70743	3	745.69143	73.946838
Residual	110.92571	11	10.084156	

First order equation

$$fd = 1.22267 + .11615w$$

Regression	214.91105	2	1074.5553	64.833317
Residual	198.88946	12	16.574121	

References

(1) G. Vieregge, "Zerspanung der Eisenwerkstoffe", Verlag Stahleisen M.B.H./Dussetdorf, 1959.

(2) L. V. Colwell, "Resume and Critique of Papers in Part Two", International Research in Production Engineering, The American Society of Mechanical Engineers, p. 140.

(3) E. M. Trent, "Some Factors Affecting Wear on Cemented Carbide Tools", The Institution of Mechanical Engineers - Proceeding (A), January - December 1952, Volume 166, pp. 64-74.

(4) Paul H. Black, Theory of Metal Cutting, New York: McGraw-Hill Book Company, Inc., 1961, p. 129.

(5) B. T. Chao and K. J. Trigger, "Temperature Distribution at Tool-chip and Tool-work Interface in Metal Cutting", Transactions of the ASME, January, 1951, Vol. 73, No. 1, p. 77.

(6) B. T. Chao and K. J. Trigger, "Controlled Contact Cutting Tools", Journal of Engineering for Industry, ASME, 1959, pp. 139-151.

(7) P. Schwartzkoph and R. Kieffer, Cemented Carbides, New York: The Macmillan Company, 1960, p. 308.

(8) B. T. Chao and K. J. Trigger, "Thermophysical Aspects of Metal Cutting", Transactions of the ASME, 1952, Vol. 74, pp. 1039-1054.

(9) B. T. Chao and K. J. Trigger, "The Mechanism of Crater Wear of Cemented Carbide Tools", Transactions of the ASME, 1956, Vol. 78, pp. 1119-1126.

Vita

John J. Burbridge, Jr. was born in Jersey City, New Jersey on December 14, 1940. He is the son of Mr. and Mrs. John J. Burbridge, Sr. He entered Lehigh University in September, 1958 and graduated in June, 1962 with a Bachelor of Science in Industrial Engineering. After graduation he worked as an industrial engineer with the Eastman Kodak Company in Rochester, New York. In September 1962, he left Eastman Kodak to return to Lehigh University. He is a member of Alpha Pi Mu, the Industrial Engineering Honor Society.